Proceedings of the ASME 2016 Heat Transfer Summer Conference
HT2016
July 10-14, 2016, Washington, DC, USA

HT2016-7413

EFFECT OF PARTICLE SIZE AND AGGREGATION ON THERMAL CONDUCTIVITY OF METAL-POLYMER NANOCOMPOSITE

Xiangyu Li, Wonjun Park, Yong P. Chen, Xiulin Ruan
Purdue University
West Lafayette, Indiana 47907

ABSTRACT

Metal nanoparticle has been a promising option for fillers in thermal interface materials due to its low cost and ease of fabrication. However, nanoparticle aggregation effect is not well understood because of its complexity. Theoretical models, like effective medium approximation model, barely cover aggregation effect. In this work, we have fabricated nickel-epoxy nanocomposites and observed higher thermal conductivity than effective medium theory predicts. Smaller particles are also found to show higher thermal conductivity, contrary to classical models indicate. A two-level EMA model is developed to account for aggregation effect and to explain the size-dependent enhancement of thermal conductivity by introducing local concentration in aggregation structures.

NOMENCLATURE

b Half width of metal line
C_{rt} Coefficient between resistance and temperature
D Thermal diffusivity
k Thermal conductivity
k_c Cluster thermal conductivity
k_e Overall thermal conductivity
k_m Matrix thermal conductivity
k_p Particle thermal conductivity
p Power consumption of metal line in 3ω*measurement*
q^{-1} penetration depth
$v_{1\omega}$ Voltage signal of ω frequency
$v_{3\omega}$ Voltage signal of 3ω frequency
ΔT Temperature oscillation amplitude
ϕ Volume concentration
ϕ_c Cluster concentration in matrix
ϕ_l Local volume concentration in agglomeration
ω Frequency of current in 3ω measurement

INTRODUCTION

Including metal nanoparticles in polymers, such as epoxy, helps to enhance thermal conductivity and to maintain electrical insulation at the same time. Because of the low cost of fabrication, metal-epoxy composite has been a great option for thermal interfacial material in many applications [1]. Aggregation effect is often observed in nanocomposites and attributed as a dominant factor in thermal conductivity enhancement [2–10]. However, its complex morphology posts a great challenge for nanocomposite design and theoretical modeling.

To estimate overall thermal conductivity with fillers, many effective medium approximation models are proposed and reviewed [11–13]. The Maxwell model assumes isolated and spherical particles in matrix material, neglecting any interactions between particles [14, 15]. Several modifications, such as the Hamilton model [16] and modified effective medium approximation [17], include a geometry factor of fillers, interfacial resistance and size effect both in filler and matrix material. Utilizing Green's function, Nan has developed a model that treats filler aspect ratio, orientation, and interfacial resistance [18]. However, these models only consider isolated particles, while aggregation effect remains neglected. The Series and Parallel models [19] consider the most simplified geometry of multi-film stacked together. The Bruggeman model [20] was developed for powder

compact, and it neglects the effect of continuous phase of the matrix material. Therefore, the Bruggeman model provides a much lower thermal conductivity when interfacial resistance is considered. The Percolation model [21] for thermal conductivity does include interactions between particles and distinguish particles and matrix, with percolation threshold and percolation exponent as two fitting parameters. Compared with electrical properties in metal-polymer composites, thermal transport does not show an increase in conductivity as dramatic as electrical conductivity [21–23]. Thus, fitting parameters can be sensitive to experimental data. Some methods for nanofluid utilize hierachical EMA models to include the aggregation effect [24] by using fractal dimensions, which can be difficult to determine [22, 25, 26] especially for nanocomposite. The Backbone method is another three-level homogenization model developed by Prasher, etc [27, 28]. It relies on two predetermined fractal dimensions. However, it still fails to fit against our experimental data of nanocomposites. Other modeling methods, such as Monte Carlo, BTE, or MD, are limited to simple periodic geometries due to their high computing cost [29].

In our work, we have fabricated nickel nanoparticle-epoxy nanocomposites and observed that they show higher thermal conductivity than effective medium theory predicts even at low concentrations below the percolation threshold. Furthermore, larger enhancement in thermal conductivity is obtained with smaller nanoparticles at the same concentration, contrary to what classical EMA models predict. Thermal conductivity characterization is done by 3ω method, and microscopy analysis by TEM indicates thermal conductivity enhancement and size-dependency are caused by the aggregation effect. A two-level effective medium approximation model is developed to consider inhomogeneous dispersion of nanoparticles, by distinguishing local and global concentrations. A rough estimation of the local concentration can be also gained with TEM figures, matching reasonably well with modeling results. Overall, the new two-level EMA model helps explain aggregation effect in nanocomposite and the size-dependent thermal conductivity enhancement, which other EMA models fail to explain.

SAMPLE FABRICATION

Nickel particles of multiple sizes 10nm, 20nm, 70nm, and 1.5μm are used to make nanocomposites. 10nm nickel particles are purchased through mkNano Inc, and other nickel particles are from Skyspring Nanomaterials. Matrix materials consist of epon 862, epikure W, both purchased from Miller-Stephenson, and curing accelerator epikure 3253 for preventing particle precipitation provided by Matteson-Ridolfi, Inc. Nickel particles, epoxy resin, curing agent, and accelerator are mixed together in THINKY mixer ARE-310 for 10 minutes. The mixture is degassed for one hour, then poured into aluminum mold. Releasing agents are sprayed ahead of time to ensure an easier removal of samples. The curing procedure occurs in an oven, with 30min temperature ramp from room temperature to 121°C with 2h hold, followed by a 30min ramp from 121°C to 177°C and 2h hold, and then a slow cooldown to room temperature [30].

The samples produced are pellets of 2.5mm thickness and 1.5cm in diameter. The top and bottom surfaces are polished to avoid contamination from releasing agent, and to make the surfaces smooth for 3ω measurements. The density is measured before and after polishing to ensure that the volume concentration of nickel is consistent.

THERMAL CONDUCTIVITY CHARACTERIZATION

Thermal conductivity is measured by the 3ω method [31, 32]. It requires a thin metal line on the surface of the sample, functioning both as a heater and detector. A metal line of 4mm long and 40μm wide is deposited on the surface of the sample with shadow mask, consisting of 20nm Cr and 150nm Au. Because of the micro-scale size of the metal line, radiation loss even at high temperature is insignificant. There have been different variations of this method to measure thin films, fluid, multilayer films, anisotropic thermal conductivity materials, etc [33, 34]. During the measurement, an AC current of frequency ω is applied to the metal line, heating up the surface of the sample with a temperature oscillation amplitude ΔT. A voltage of 3ω frequency is also present across the metal line. Detailed deductions about ΔT can be found in previous literatures [31, 32] as

$$\Delta T = \frac{2v_{3\omega}}{v_{1\omega}C_{rt}} = \frac{p}{\pi k}\int_0^\infty \frac{sin^2(\lambda b)}{(\lambda b)^2(\lambda^2+2i\omega/D)^{1/2}}d\lambda. \quad (1)$$

By measuring $v_{1\omega}$, $v_{3\omega}$, and temperature coefficient of resistance C_{rt} of the metal line, thermal conductivity of nanocomposites can be obtained by fitting real and imaginary part of theoretical $\Delta T/p$ to experimental in-phase and out-of-phase signal respectively. A typical fitting procedure on one of our Ni-epoxy nanocomposite samples is shown in Fig. 1, with thermal conductivity obtained as 0.28W/mK.

The thermal conductivities of nanocomposites with different nickel particle sizes and volume concentrations are shown in Fig. 2, where the Maxwell model curve is also plotted. Without the inclusion of interfacial resistance, the thermal conductivity from the Maxwell model is independent on particle sizes. All of the thermal conductivities are higher than the Maxwell model predicts. Surprisingly, it is also observed that smaller fillers provide higher thermal conductivity at the same concentration, contrary to the trend of classical EMA models, where thermal conductivity decreases with smaller particles due to interfacial resistance. Motivated by these observations, we slice our composites samples into 100nm thickness and characterize the microscopy structure with transmission electron microscopy(TEM). According to Fig. 3, nickel particles (dark dots), are not isolated or

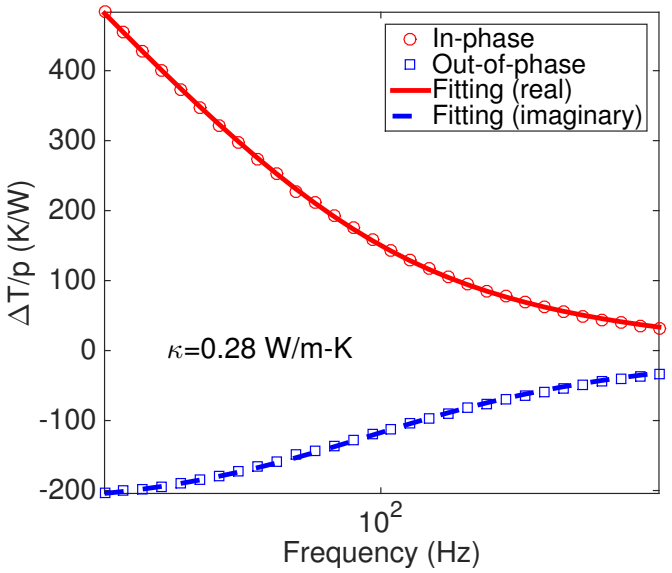

FIGURE 1: 3ω MEASUREMENT DATA FOR NI-EPOXY NANOCOMPOSITE

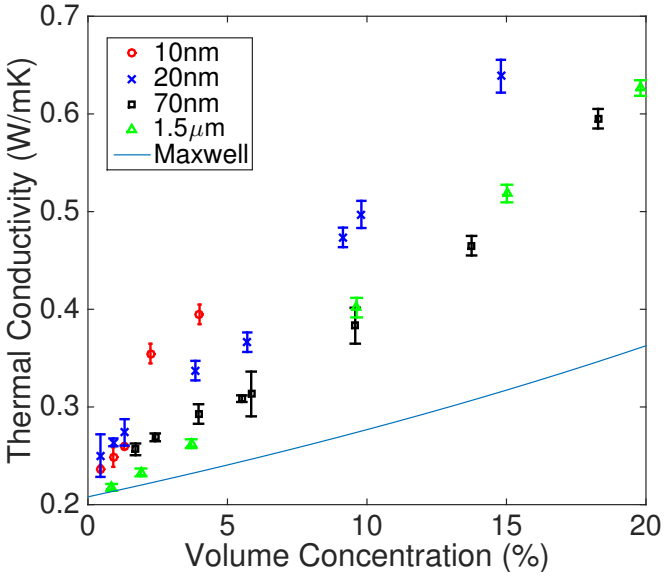

FIGURE 2: THERMAL CONDUCTIVITY CHARACTERIZATION RESULTS OF NI-EPOXY NANOCOMPOSITES

located evenly. Instead, they aggregate to form some clusters with high local concentration. Interactions between particles help form a continuous path to conduct heat better within nickel phase, thus increase the overall thermal conductivity more effectively than isolated dispersion. On the other hand, these clusters are mostly isolated from each other. It is also important to note that 20nm nanoparticles form a more spread-out cluster structure than 70nm, which is likely the reason for size-dependent thermal conductivity. In this case, using a single-level EMA model like the Maxwell model would ignore the aggregation effect. On the other hand, although the percolation model considers the aggregation effect, it does not treat the nonuniform particle distribution. In this work, a 2-level EMA is developed to account for the aggregation effect.

TWO-LEVEL EMA MODELING

Our 2-level EMA model adopts a different EMA model at each level, shown in Fig. 4. The first level is a cluster where nanoparticles are packed closely, and the second level is the whole composite where each cluster is treated as an isolated new particle. A local concentration, ϕ_l, is defined as the concentration of particles inside clusters. The cluster concentration ϕ_c, is defined as volume concentration of clusters inside the matrix material. Thus the overall concentration of nanoparticles will be preserved as $\phi = \phi_l \times \phi_a$. For the first level EMA, where particles are packed together, the Hashin and Shtrikman model is used as

$$k_c = k_p \frac{2\phi_l}{3-\phi_l}, \tag{2}$$

where k_p is nickel particle thermal conductivity, ϕ_l is the local volume concentration, k_c is the thermal conductivity of clusters. Several attempts in literature have shown that with sufficient particle interactions at high concentration, thermal conductivity enhancement can be comparable to the higher bound of the Hashin and Shtrikman model [5–9,35]. On the second level, even though the aggregation structures appear as cylinders, rods, and some irregular shapes in TEM images, the true geometry factor remains uncertain. The TEM figures only show a slice of 100nm thickness, thus those agglomerations that seem to be connected together might be relatively distant away, and some small agglomerations might be only part of larger ones. Because of spherical particles and isolated clusters, we assume spherical agglomerations based on the Maxwell model as

$$k_e = k_m \frac{k_c + 2k_m + 2\phi_c(k_c - k_m)}{k_c + 2k_m - \phi_c(k_c - k_m)}, \tag{3}$$

where k_c is the thermal conductivity of clusters, k_e is effective thermal conductivity of nanocomposites, k_m is matrix thermal

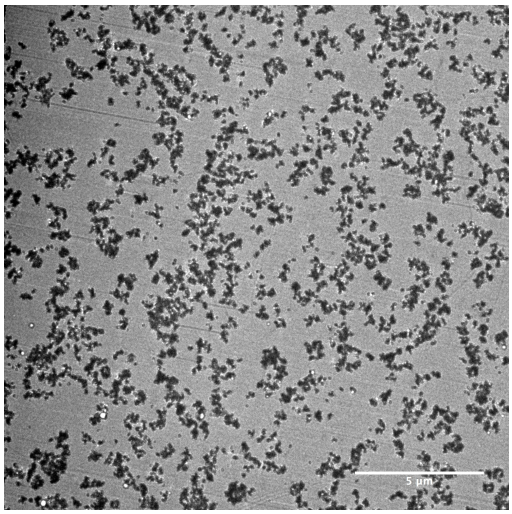

(a) NANOCOMPOSITE WITH 20NM NI AT 5.74%

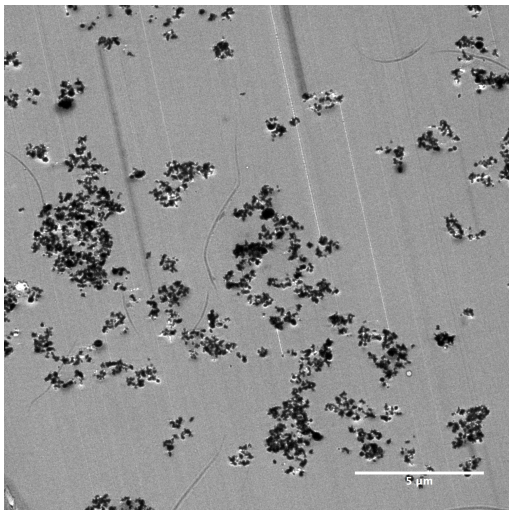

(b) NANOCOMPOSITE WITH 70NM NI AT 5.52%

FIGURE 3: TEM FIGURES OF NANOCOMPOSITE WITH 20NM AND 70NM NICKEL PARTICLES

conductivity, and ϕ_c is the volume concentration of clusters in epoxy. If the aspect ratio is to be measured or fitted in the model, Nan's model can be an alternative model to include the geometry factor.

The local concentration ϕ_l of each sample is fitted with experimental data, and plotted in Fig. 5, where the curve $\phi_l = \phi$ is also included for comparison. All local concentrations are above the curve $\phi_l = \phi$, indicating higher local concentrations in clusters. For smaller particles as 10nm, 20nm, 70nm at low concentrations, the local concentration increases faster than overall concentration does. In other words, particles tend to aggregate more closely with higher particle loadings. After certain

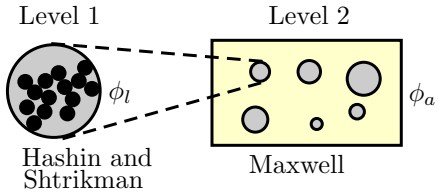

FIGURE 4: 2-LEVEL EMA MODEL

TABLE 1: COMPARISON BETWEEN TWO NANOCOMPOSITES

Particle size	ϕ	ϕ_l	ϕ_c	k_c^*	k_e^*
20nm	5.74%	27%	21.6%	18.2	0.37
70nm	5.52%	39%	14.2%	27.3	0.31

* W/mK

concentration, the local concentration increasing speed becomes similar to that of overall concentration. It is interesting to note that with a lower local concentration, overall thermal conductivity tends to be higher at the same overall concentration. A comparison is made between 20nm sample at 5.74% and 70nm sample at 5.52% in Tab. 1. Even though 70nm nanocomposite has a higher local concentration, thus a higher cluster thermal conductivity, its lower cluster concentration limits its overall thermal conductivity. Referring to Fig. 3 at similar concentrations and the same magnification, aggregation structure of 20nm nanoparticles is more beneficial for heat transfer, since clusters are more spread-out and extensive, which translates into larger ϕ_c or smaller ϕ_l. Thus, aggregation effect enhances thermal conductivity compared with isolated particle dispersion, and an extensive aggregation structure or low local concentration is preferred for higher thermal conductivity. The local concentration of 1.5μm is less dependent on overall concentration mainly because of its much larger size compared with other nanoparticles, thus smaller number of particles and longer distance between them.

Besides fitting to the thermal conductivities of experimental data, the local concentrations of nickel particles in clusters can also be roughly estimated from TEM images by evaluating cluster concentration in matrix ϕ_c first. The method is to assume the particle distribution to be uniform along with the 100nm thickness of TEM slice. Then the ratio of area occupied by closely packed particle to the total area is ϕ_c. Using the overall concentration of particles ϕ, the local concentration ϕ_l can be estimated. Figure 3 contains two TEM pictures of 20nm nickel and 70nm nickel at similar volume concentrations. The local concentration of these two samples are calculated to be $13.1\% \pm 0.2\%$,

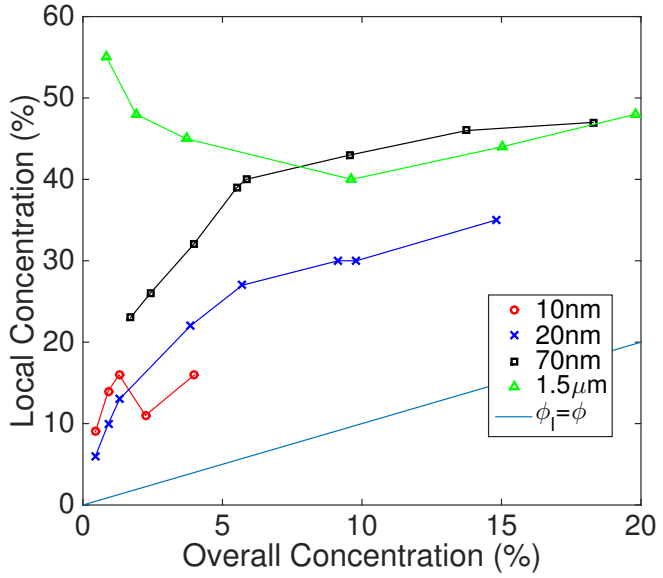

FIGURE 5: LOCAL CONCENTRATION OF NI PARTICLES IN AGGREGATIONS

and $23.9 \pm 1.8\%$, respectively, comparing to the fitted local concentrations 27% and 39%. This is probably because that the assumption that the particle dispersion is uniform across 100nm overestimates ϕ_c, thus underestimates ϕ_l. Nonetheless, the estimations based on the TEM images still follow the same trend with those fitted from our 2-level EMA model.

The backbone method is another hierarchical EMA model, proposed by Prasher, estimating thermal conductivity of nanofluid including the aggregation effect [27,28]. Three parameters are needed as overall fractal dimension, backbone fractal dimension, and gyration radius. Overall fractal dimension is usually set as 1.7 for nanofluids and 2.0 for nanocomposites [25,26]. However, the model cannot achieve thermal conductivity as high as our experimental results, even by setting gyration radius as a parameter.

CONCLUSION

In this work, we observe higher thermal conductivity of nickel-epoxy nanocomposites compared with other EMA models predict, due to aggregation effect. At the same concentration, smaller particle size shows higher thermal conductivities due to its wider-spread aggregation structures in epoxy, according to TEM figures. A two-level EMA model with the local concentration as a fitting parameter indicates a lower local concentration for smaller particles, thus a higher effective thermal conductivity. Local concentration for nanoparticles also shows an increasing trend with higher overall concentration, and saturates later. An estimation of local concentration based on TEM figures follows the trend and agrees reasonably well with modeling results. Overall, the new two-level EMA model works well with nanocomposites, and helps explain the aggregation effect and size dependent thermal conductivity enhancement.

ACKNOWLEDGMENT

We acknowledge the financial support from the Cooling Technologies Research Center, a University/Industry Cooperative Research Center. We also thank the help from Jennifer Case and Professor Rebecca Kramer on the sample fabrication.

REFERENCES

[1] B, E., 1993. *Chemistry and technology of epoxy resins*. New York, NY: Blackie Academic & Professional.

[2] Hsu, S. H., Chou, C. W., and Tseng, S. M., 2004. "Enhanced thermal and mechanical properties in polyurethane/Au nanocomposites". *Macromolecular Materials and Engineering,* ***289***(12), pp. 1096–1101.

[3] Karthikeyan, N., Philip, J., and Raj, B., 2008. "Effect of clustering on the thermal conductivity of nanofluids". *Materials Chemistry and Physics,* ***109***(1), may, pp. 50–55.

[4] Pardiñas-Blanco, I., Hoppe, C. E., López-Quintela, M., and Rivas, J., 2007. "Control on the dispersion of gold nanoparticles in an epoxy network". *Journal of Non-Crystalline Solids,* ***353***(8-10), apr, pp. 826–828.

[5] Philip, J., Shima, P. D., and Raj, B., 2008. "Evidence for enhanced thermal conduction through percolating structures in nanofluids.". *Nanotechnology,* ***19***(30), p. 305706.

[6] Philip, J., Shima, P. D., and Raj, B., 2008. "Nanofluid with tunable thermal properties". *Applied Physics Letters,* ***92***(4), pp. 2–5.

[7] Philip, J., Shima, P. D., and Raj, B., 2007. "Enhancement of thermal conductivity in magnetite based nanofluid due to chainlike structures". *Applied Physics Letters,* ***91***(20), pp. 2–5.

[8] Reinecke, B. N., Shan, J. W., Suabedissen, K. K., and Cherkasova, A. S., 2008. "On the anisotropic thermal conductivity of magnetorheological suspensions". *Journal of Applied Physics,* ***104***(2).

[9] Wu, S., Ladani, R. B., Zhang, J., Kinloch, A. J., Zhao, Z., Ma, J., Zhang, X., Mouritz, A. P., Ghorbani, K., and Wang, C. H., 2015. "Epoxy nanocomposites containing magnetite-carbon nanofibers aligned using a weak magnetic field". *Polymer,* ***68***, pp. 25 – 34.

[10] Zhu, H., Zhang, C., Liu, S., Tang, Y., and Yin, Y., 2006. "Effects of nanoparticle clustering and alignment on thermal conductivities of fe3o4 aqueous nanofluids". *Applied Physics Letters,* ***89***(2).

[11] Lee, J.-H., Lee, S.-H., Choi, C. J., Jang, S. P., and Choi, S.

U. S., 2011. "A Review of Thermal Conductivity Data, Mechanisms and Models for Nanofluids". *International Journal of Micro-Nano Scale Transport,* ***1***(4), pp. 269–322.

[12] Lee, S., Cahill, D. G., and Allen, T. H., 1995. "Thermal conductivity of sputtered oxide film". *Physical Review B,* ***52***(1), pp. 253–257.

[13] Wang, M., and Pan, N., 2008. "Predictions of effective physical properties of complex multiphase materials". *Materials Science and Engineering: R: Reports,* ***63***(1), dec, pp. 1–30.

[14] Maxwell, J., 1954. *A treatise on electricity and magnetism*. Dover Publications.

[15] Garnett, J. C. M., 1906. "Colours in Metal Glasses, in Metallic Films, and in Metallic Solutions. II". *Philosophical Transactions of the Royal Society A: Mathematical, Physical and Engineering Sciences,* ***205***(387-401), pp. 237–288.

[16] Hamilton, R. L., and Crosser, O. K., 1962. "Thermal conductivity of heterogeneous two-component systems". *Industrial & Engineering Chemistry Fundamentals,* ***1***(3), pp. 187–191.

[17] Minnich, A., and Chen, G., 2007. "Modified effective medium formulation for the thermal conductivity of nanocomposites". *Applied Physics Letters,* ***91***(7), p. 073105.

[18] Nan, C.-W., Birringer, R., Clarke, D. R., and Gleiter, H., 1997. "Effective thermal conductivity of particulate composites with interfacial thermal resistance". *Journal of Applied Physics,* ***81***(10), p. 6692.

[19] Eucken, A., 1932. "Thermal conductivity of ceramic refractory materials: calculation from thermal conductivities of constituents". *Forsch. Gebiete Ingenieurw,* ***B3(353)***, p. 16.

[20] Landauer, R., 1952. "The electrical resistance of binary metallic mixtures". *Journal of Applied Physics,* ***23***(7), pp. 779–784.

[21] Guoqing Zhang, Yanping Xia, Hui Wang, Yu Tao, Guoliang Tao, Shantung Tu, and Haiping Wu, 2010. "A Percolation Model of Thermal Conductivity for Filled Polymer Composites". *Journal of Composite Materials,* ***44***(8), pp. 963–970.

[22] Nan, C.-W., 1993. "Physics of inhomogeneous inorganic materials". *Progress in Materials Science,* ***37***(1), pp. 1 – 116.

[23] Nan, C.-W., Shen, Y., and Ma, J., 2010. "Physical Properties of Composites Near Percolation". *Annual Review of Materials Research,* ***40***(1), pp. 131–151.

[24] Wang, B. X., Zhou, L. P., and Peng, X. F., 2003. "A fractal model for predicting the effective thermal conductivity of liquid with suspension of nanoparticles". *International Journal of Heat and Mass Transfer,* ***46***(14), pp. 2665–2672.

[25] Meakin, P., Majid, I., Havlin, S., and Stanley, H. E., 1999. "Topological properties of diffusion limited aggregation and cluster-cluster aggregation". *Journal of Physics A: Mathematical and General,* ***17***(18), pp. L975–L981.

[26] Meakin, P., 1987. "Fractal aggregates". *Advances in Colloid and Interface Science,* ***28***, pp. 249–331.

[27] Prasher, R., Evans, W., Meakin, P., Fish, J., Phelan, P., and Keblinski, P., 2006. "Effect of aggregation on thermal conduction in colloidal nanofluids". *Applied Physics Letters,* ***89***(14), pp. 1–4.

[28] Evans, W., Prasher, R., Fish, J., Meakin, P., Phelan, P., and Keblinski, P., 2008. "Effect of aggregation and interfacial thermal resistance on thermal conductivity of nanocomposites and colloidal nanofluids". *International Journal of Heat and Mass Transfer,* ***51***(5-6), mar, pp. 1431–1438.

[29] Chen, G., 1998. "Thermal conductivity and ballistic-phonon transport in the cross-plane direction of superlattices". *Physical Review B,* ***57***(23), jun, pp. 14958–14973.

[30] Chen, C., and Curliss, D., 2003. "Evolution of Epoxy Nanocomposites". *Applied of Polymer Science,* ***2***(1).

[31] Cahill, D. G., 1990. "Thermal conductivity measurement from 30 to 750 K: the 3ω method". *Review of Scientific Instruments,* ***61***(2), p. 802.

[32] Cahill, D. G., 1989. "Thermal conductivity of thin films: Measurements and understanding". *Journal of Vacuum Science & Technology A: Vacuum, Surfaces, and Films,* ***7***(3), may, p. 1259.

[33] Bodenschatz, N., Liemert, A., Schnurr, S., Wiedwald, U., and Ziemann, P., 2013. "Extending the 3ω method: Thermal conductivity characterization of thin films". *Review of Scientific Instruments,* ***84***(8).

[34] Borca-Tasciuc, T., Kumar, a. R., and Chen, G., 2001. "Data reduction in 3ω method for thin-film thermal conductivity determination". *Review of Scientific Instruments,* ***72***(4), p. 2139.

[35] Pashayi, K., Fard, H. R., Lai, F., Iruvanti, S., Plawsky, J., and Borca-Tasciuc, T., 2012. "High thermal conductivity epoxy-silver composites based on self-constructed nanostructured metallic networks". *Journal of Applied Physics,* ***111***(10), p. 104310.